Magnetic Properties of Nanostructured Materials

Diandra L. Leslie-Pelecky

Center for Materials Research & Analysis, Department of Physics & Astronomy, University of Nebraska, Lincoln, Nebraska 68588-0111

Reuben D. Rieke

Center for Materials Research & Analysis, Department of Chemistry, University of Nebraska, Lincoln, Nebraska 68588-0304

Received February 1, 1996[⊗]

Understanding the correlation between magnetic properties and nanostructure involves collaborative efforts between chemists, physicists, and materials scientists to study both fundamental properties and potential applications. This article introduces a classification of nanostructure morphology according to the mechanism responsible for the magnetic properties. The fundamental magnetic properties of interest and the theoretical frameworks developed to model these properties are summarized. Common chemical and physical techniques for the fabrication of magnetic nanostructures are surveyed, followed by some examples of recent investigations of magnetic systems with structure on the nanometer scale. The article concludes with a brief discussion of some promising experimental techniques in synthesis and measurements.

I. Introduction

The term "nanostructured" (NS) describes materials with structure on length scales from 1 to 100 nm. NS materials often have unique electrical, chemical, structural, and magnetic properties,[1−9] with potential applications including: information storage,[10] color imaging, bioprocessing, magnetic refrigeration,[11,12] and ferrofluids.[13−16] Nanostructured materials exhibit a unique type of disorder, with very-low-energy regions (crystallites) existing at the expense of higher-energy boundary, interface, or surface regions. Gleiter[3] calls this "heterogeneous disorder", in contrast to the homogeneous disorder of structural glasses.

Magnetic nanoparticle and nanostructure studies combine a broad range of synthetic and investigative techniques from physics, chemistry, and materials science. In the best case, these studies provide not only information about the structural and magnetic properties of the materials but also improve understanding of the synthesis technique. This paper reviews recent progress in the synthesis and understanding of nanostructured magnetic systems. After a short explanation of magnetic units, we propose a scheme for the classification of nanostructure morphology as a function of magnetic interaction. A theoretical section provides the motivation for fabricating nanostructured magnetic materials, introduces the physical properties of interest in magnetism, and discusses theoretical schemes developed to explain nanoscale magnetism. The third section contains the experimental results and is divided into two parts. The first part surveys frequently used fabrication techniques and their applicability to the different classes of materials, while the second part highlights some of the most interesting recent results. The paper concludes by identifying some promising areas for future developments in the production and measurement of this interesting class of materials.

A. Units.

The wide range of scientists and engineers working in magnetic nanostructured materials has resulted in a curious mix of units in the literature. Papers describing engineering applications usually use SI units. More fundamental reports—including this one—rely on cgs units, in which magnetization, M, is measured in emu/cm^3 (electromagnetic units), magnetic field strength, H, is measured in Oe (Oersted), and the permeability of vacuum is taken as unity. The relationship between magnetic induction (B), magnetic field strength (H), and magnetization (M) is given by $B = H + 4\pi M$, with B in gauss. Scholten provides a convenient overview of the various magnetic unit conventions.[17]

B. Classification.

The correlation between nanostructure and magnetic properties suggests a classification of nanostructure morphologies. Although other schemes have been proposed,[2] the following classification is designed to emphasize the physical mechanisms responsible for the magnetic behavior. At one extreme are systems of isolated particles with nanoscale diameters, which are denoted type A. These noninteracting systems derive their unique magnetic properties strictly from the reduced size of the components, with no contribution from interparticle interactions. At the other extreme are bulk materials with nanoscale structure (type D) in which a significant fraction (up to 50%) of the sample volume is composed of grain boundaries and interfaces. In contrast to type-A systems, magnetic properties here are dominated by interactions. The length scale of the interactions can span many grains[18] and is critically dependent on the character of the interphase. The dominance of interactions and grain boundaries in type-D nanostructures means that magnetic behavior cannot be predicted simply by applying theories for polycrystalline materials with reduced length scales.

[⊗] Abstract published in *Advance ACS Abstracts,* July 15, 1996.

S0897-4756(96)00077-4 CCC: $12.00

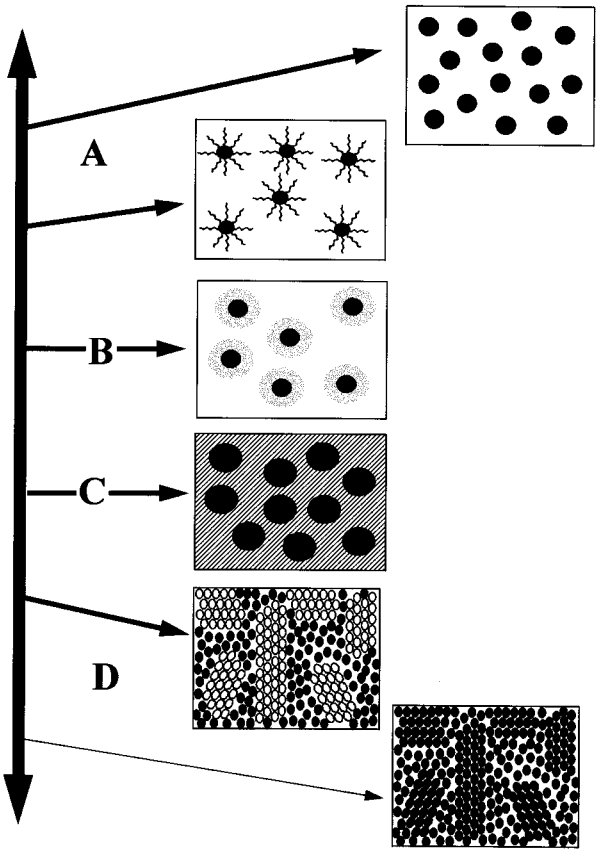

Figure 1. Schematic representation of the different types of magnetic nanostructures. Type-A materials include the ideal ultrafine particle system, with interparticle spacing large enough to approximate the particles as noninteracting. Ferrofluids, in which magnetic particles are surrounded by a surfactant preventing interactions, are a subgroup of Type-A materials. Type-B materials are ultrafine particles with a core-shell morphology. Type-C nanocomposites are composed of small magnetic particles embedded in a chemically dissimilar matrix. The matrix may or may not be magnetoactive. Type-D materials consists of small crystallites dispersed in a noncrystalline matrix. The nanostructure may be two-phase, in which nanocrystallites are a distinct phase from the matrix, or the ideal case in which both the crystallites and the matrix are made of the same material.

The magnetic behavior of most experimentally realizable systems is a result of contributions from both interaction and size effects. For structural properties, classification of materials according to dimensionality is useful;[2] however, for magnetic systems, an alternative scheme is suggested. Figure 1 schematically illustrates four classifications of magnetic nanostructured materials ranging from noninteracting particles (type A) in which the magnetization is determined strictly by size effects, to fine-grained nanostructures, in which interactions dominate the magnetic properties. Two forms of each of these types are indicated: the ideal type A material is one in which the particles are separated and can be treated as noninteracting. Ferrofluids, in which long surfactant molecules provide separation of particles, are a subset of type A. Type-D materials may be single phase, in which both the crystallites and the noncrystalline material are chemically identical, or they may be multiple phase. Intermediate forms include ultrafine particles with a core-shell morphology (type B), as well as nanocomposite materials (type C) in which two chemically dissimilar materials are combined. In type-B particles, the presence of a shell can help prevent particle−particle interactions, but often at the cost of interactions between the core and the shell. In many cases, the shells are formed via oxidation and may themselves be magnetic. Type-C nanocomposites consist of magnetic particles distributed throughout a matrix, and the magnetic interactions are determined by the volume fraction of the magnetic particles and the character of the matrix.

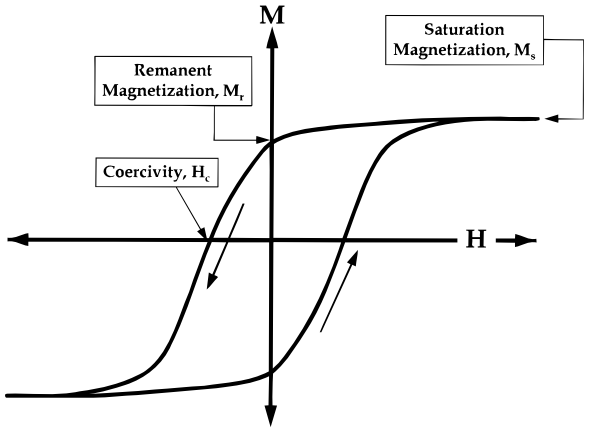

Figure 2. Important parameters obtained from a magnetic hysteresis loop. The saturation magnetization, M_s, remanent magnetization, M_r, and coercivity, H_c, are shown.

II. Theoretical Background

A. Motivation. The fundamental motivation for the fabrication and study of nanoscale magnetic materials is the dramatic change in magnetic properties that occurs when the critical length governing some phenomenon (magnetic, structural, etc.) is comparable to the nanoparticle or nanocrystal size. Effects due to surfaces or interfaces are stronger in particulate systems than in thin films due to the larger amount of surface.

Changes in the magnetization of a material occur via activation over an energy barrier. Each physical mechanism responsible for an energy barrier has an associated length scale. The fundamental magnetic lengths[19] are the crystalline anisotropy length, l_K, the applied field length, l_H, and the magnetostatic length, l_S, which are defined in eqs 1:

$$l_K = \sqrt{J/K} \tag{1a}$$

$$l_H = \sqrt{2J/HM_S} \tag{1b}$$

$$l_S = \sqrt{J/2\pi M_S^2} \tag{1c}$$

K is the anisotropy constant of the bulk material due to the dominant anisotropy (see section II.B) and J is the exchange within a grain. If more than one type of barrier is present, magnetic properties are dominated by the shortest characteristic length. For most common magnetic materials, these lengths are on the order of 1−100 nm. For example, nickel at 1000 Oe and room temperature has lengths $l_S \cong 8$ nm, $l_K \cong 45$ nm, and $l_H \cong 19$ nm.

To familiarize the reader with commonly measured magnetic parameters, Figure 2 schematically illustrates a hysteresis loop (magnetization vs field). The application of a sufficiently large magnetic field causes the

spins within a material to align with the field. The maximum value of the magnetization achieved in this state is called the saturation magnetization, M_s. As the magnitude of the magnetic field decreases, spins cease to be aligned with the field, and the total magnetization decreases. In ferromagnets, a residual magnetic moment remains at zero field. The value of the magnetization at zero field is called the remanent magnetization, M_r. The ratio of the remanent magnetization to the saturation magnetization, M_r/M_s, is called the remanence ratio and varies from 0 to 1. The coercive field H_c is the magnitude of the field that must be applied in the negative direction to bring the magnetization of the sample back to zero. The shape of the hysteresis loop is especially of interest for magnetic recording applications, which require a large remanent magnetization, moderate coercivity, and (ideally) a square hysteresis loop.

B. Anisotropy. Most materials contain some type of anisotropy affecting the behavior of the magnetization. The most common types of anisotropy are (1) crystal anisotropy, (2) shape anisotropy, (3) stress anisotropy, (4) externally induced anisotropy, and (5) exchange anisotropy.[20] The two most common anisotropies in nanostructured materials are crystalline and shape anisotropy. The anisotropy can often be modeled as uniaxial in character and represented by (in its simplest form)

$$E = KV \sin^2 \theta \qquad (2)$$

where K is the effective uniaxial anisotropy energy per unit volume, θ is the angle between the moment and the easy axis, and V is the particle volume.

Magnetocrystalline anisotropy arises from spin−orbit coupling and energetically favors alignment of the magnetization along a specific crystallographic direction. The direction favored by the magnetocrystalline anisotropy is called the easy axis of the material. The magnetocrystalline anisotropy is specific to a given material and independent of particle shape. In hcp cobalt, magnetocrystalline anisotropy causes the magnetization to point along the *c* axis. In cubic systems (such as Fe and Ni) symmetry creates multiple easy axes. In nickel, the ⟨111⟩ axes are the easy axes, while the ⟨100⟩ axes are the easy axes in iron. The magnitude of the magnetocrystalline anisotropy at room temperature is 7×10^6 erg/cm^3 in Co, 8×10^5 erg/cm^3 in Fe, and 5×10^4 erg/cm^3 in Ni. The coercivity is proportional to the anisotropy constant, so high-anisotropy materials (such as rare-earth cobalts, which have anisotropies approaching 10^8 erg/cm^3) are attractive candidates for high-coercivity applications.

A polycrystalline sample with no preferred grain orientation has no net crystal anisotropy due to averaging over all orientations. A nonspherical polycrystalline specimen can possess shape anisotropy. A cylindrical sample, for example, is easier to magnetize along the long direction than along the short directions. A symmetric shape, such as a sphere, will have no net shape anisotropy.

Stress anisotropy is the result of external or internal stresses due to rapid cooling, application of external pressure, etc. Anisotropy may also be induced by annealing in a magnetic field, plastic deformation, or ion beam irradiation. Exchange anisotropy occurs when a ferromagnet is in close proximity to an antiferromagnet or ferrimagnet. Magnetic coupling at the interface of the two materials can create a preferential direction in the ferromagnetic phase, which takes the form of a unidirectional anisotropy.[21−23] This type of anisotropy is most often observed in type-B particles when an antiferromagnetic or ferrimagnetic oxide forms around a ferromagnetic core.

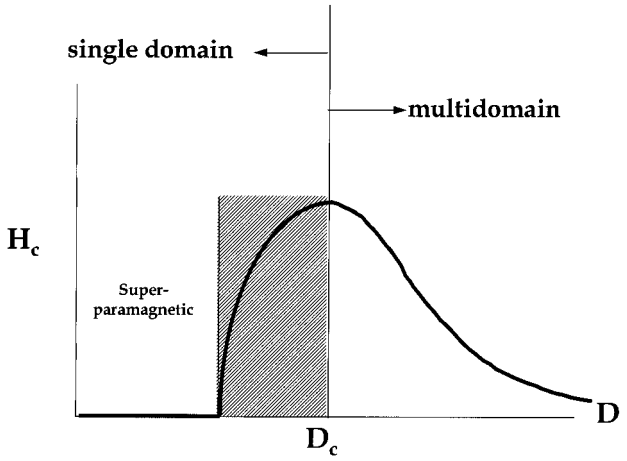

Figure 3. Qualitative illustration of the behavior of the coercivity in ultrafine particle systems as the particle size changes.

Shape anisotropy is predicted to produce the largest coercive forces. The departure from sphericity does not need to be significant: an increase in the aspect ratio from 1.1 to 1.5 in single-domain Fe particles with easy axis aligned along the field quadruples the coercivity. An increase in the aspect ratio to 5 produces another doubling of the coercivity. For comparison, a sample having the same coercivity as the 1.1 aspect ratio Fe particle would need a crystal anisotropy of 2.8×10^6 erg/cm^3 (compared to the standard value of 8×10^5 erg/cm^3).

C. Single Domain Particles. Reviews of single-domain particles include those by Bean and Livingston,[24] Bean,[25] Jacobs and Bean,[26] Brown,[27] Wohlfarth,[28] and Kneller.[29] Domains—groups of spins all pointing in the same direction and acting cooperatively—are separated by domain walls, which have a characteristic width and energy associated with their formation and existence. The motion of domain walls is a primary means of reversing magnetization. Experimental investigation[30,31] of the dependence of coercivity on particle size showed behavior similar to that schematically illustrated in Figure 3. In large particles, energetic considerations favor the formation of domain walls. Magnetization reversal thus occurs through the nucleation and motion of these walls. As the particle size decreases toward some critical particle diameter, D_c, the formation of domain walls becomes energetically unfavorable and the particles are called single domain. Changes in the magnetization can no longer occur through domain wall motion and instead require the coherent rotation of spins, resulting in larger coercivities. As the particle size continues to decrease below the single domain value, the spins are increasingly affected by thermal fluctuations and the system becomes superparamagnetic (see section II.E).

Theoretical predictions of the existence of single domain particles were made by Frenkel and Dorfman,[32]

Table 1. Estimated Single-Domain Sizes for Spherical Particles with No Shape Anisotropy

material	D_{crit} (nm)	material	D_{crit} (nm)
Co	70	Fe_3O_4	128
Fe	14	γ-Fe_2O_3	166
Ni	55		

with estimates of the critical size made by Kittel[33] and others. Table 1 estimates the single-domain diameter for some common materials in the shape of spherical particles. Note that particles with significant shape anisotropy can remain single domain to much larger dimensions than their spherical counterparts.

D. Time Dependence and Remanence. The time over which the magnetization of a system will remain in a certain state is of importance for practical engineering applications as well for probing the fundamental mechanisms of magnetization reversal.[34,35] The time variation of the magnetization of any magnetic system can be generally described by

$$\frac{dM(t)}{dt} = -\frac{M(t) - M(t=\infty)}{\tau} \tag{3}$$

where $M(t=\infty)$ is the equilibrium magnetization and τ is a characteristic relaxation time corresponding to relaxation over an energy barrier:

$$\tau^{-1} = f_0 e^{-\Delta E/kT} \tag{4}$$

For uniaxial anisotropies, the energy barrier, ΔE, is equal to the product of the anisotropy constant and the volume. f_0 is often taken as a constant of value 10^9 s^{-1},[36,37] but actually depends on applied field, particle volume, and the magnitude of the anisotropy constant.[38,39] Although some experimental studies suggest that a value of $10^{12}-10^{13}$ s^{-1} is more appropriate,[40,41] exact knowledge of the magnitude of f_0 is not necessary because the behavior of τ is dominated by the exponential argument. For measurement times between 1 and 1000 s, energy barriers with heights between 25 and 32 kT contribute to the measurement. Note also that the relaxation time depends critically on the particle size (as $\exp(d^3)$). Assuming representative values ($f_0 = 10^9$ s^{-1}, $K = 10^6$ erg/cm^3, and $T = 300$ K), a particle of diameter 11.4 nm will have a relaxation time of 0.1 s. Increasing the particle diameter to 14.6 nm increases τ to 10^8 s.

The simplest solution to eq 3 occurs when all components of a system have the same relaxation time; however, the expected behavior is not usually observed in real systems due to a distribution of energy barriers. The energy barrier distribution may be due to a variation of particle sizes, anisotropies, or compositional inhomogeneity and results in a distribution of relaxation times. If the distribution of energy barriers can be approximated as nearly constant, the magnetization decays logarithmically:[42]

$$M(t) = M(t=0) - S \ln(t) \tag{5}$$

where the magnetic viscosity, S, contains information about the energy barrier distribution. When the distribution function is not constant, deviations from logarithmic behavior are observed if the measurement extends to sufficiently long times.[43−48] Narrow energy barrier distributions are more likely to exhibit deviations from the $\ln(t)$ behavior, while systems with a wide distribution of energy barriers will obey this behavior over a longer time window. If a form for the energy barrier distribution can be assumed, S can be calculated analytically. For single-domain particles with uniaxial anisotropy

$$S = \chi_{irr}\, kT/M_s v \tag{6}$$

where χ_{irr} is the first differential of the remanence curve.[49] The activation volume, v,[50−52] is an estimate of the volume over which spins act coherently. Time-dependent measurements of the magnetization coupled with determination of χ_{irr} can thus provide an estimate of the activation volume. Coherent rotation of all spins is assumed in arriving at this expression, so the activation volume is often smaller than the physical volume of the switching unit due to incoherent reversal mechanisms.

The form of S has been analytically calculated for distributions of particle volumes,[53,54] anisotropy constants,[55] and anisotropy axes.[56] Measured as a function of field, S usually has a peak at a field near the coercivity,[59] with the maximum value of S going as $T^{1/2}$ or T.[56−59] In the special case of a log-normal distribution, the field at which the maximum value of S occurs is identical with the coercive field. An review of slow relaxation behavior was recently presented by Chantrell et al.[60]

Remanence refers to the behavior of a system after a change in the applied field. The isothermal remanent magnetization (IRM) is measured from the demagnetized state. A field is applied and removed, and the magnetization measured, which gives the IRM as a function of field, $M^{IRM}(H)$. Cooling to some temperature in a field and measuring the decay of the magnetization after the removal of the cooling field measures the thermoremanent magnetization (TRM). The dc demagnetization curve (DCD) is similar to the IRM but is measured from an initially positively saturated state. A negative field is applied and then removed, and the magnetization measured. The DCD is measured as a function of increasingly negative field until negative saturation remanence has been achieved and is denoted by $M^{DCD}(H)$. The IRM and the DCD may be normalized to their saturation values and run from 0 to +1 and +1 to −1, respectively.

E. Superparamagnetism. Néel[61] showed theoretically that H_c approaches zero for very small particles because thermal fluctuations can prevent the existence of a stable magnetization. Returning to eq 4, if we take an arbitrary measurement time to be $\tau = 100$ s and $f_0 = 10^9$ s^{-1}, then

$$\Delta E_{crit} = \ln(tf_0)kT = 25kT \tag{7}$$

For a particle with a uniaxial anisotropy, $\Delta E = KV$ (at $H = 0$) and the condition for superparamagnetism becomes

$$KV = 25kT \tag{8}$$

Again, the strong dependence on the argument of the exponential makes exact knowledge of f_0 less important. If f_0 is 10^{12} s^{-1}, the criteria becomes $KV = 32kT$. On a measuring time scale of 100 s, particles with $\Delta E > \Delta E_{crit}$ are blocked—they do not relax during the time of the measurement. A blocking temperature, T_B, can be defined as

$$T_B = \Delta E/25k \quad (9)$$

The blocking temperature in a superparamagnetic system decreases with increasing measuring fields, being proportional to $H^{2/3}$ at large magnetic fields and proportional to H^2 at lower fields.[62,63]

The temperature-dependent magnetization $M(T)$ exhibits a cusp in the zero-field-cooled (ZFC) susceptibility at the blocking temperature, T_B. Above T_B, the particles are free to align with the field during the measuring time. This state is called superparamagnetic, because the particle behaves similarly to paramagnetic spin but with a much larger moment. The magnetization of a system of particles, $\bar{\mu}$, is described by the Langevin function

$$\frac{\bar{\mu}}{\mu} = L\left(\frac{\mu H}{kT}\right) = \coth\left(\frac{\mu H}{kT}\right) - \frac{kT}{\mu H} \quad (10)$$

where μ is the magnetic moment of a single particle. At low fields ($\mu H \ll kT$), the magnetization behaves as $\mu H/3kT$ and at high fields ($\mu H \ll kT$), as $1 - kT/\mu H$. If a distribution of particle sizes is present, the initial susceptibility is sensitive to the larger particles present, and the approach to saturation is more sensitive to the smaller particles present.

The experimental criteria for superparamagnetism are (1) the magnetization curve exhibits no hysteresis and (2) the magnetization curves at different temperatures must superpose in a plot of M vs H/T.[64−66] Imperfect H/T superposition can result from a broad distribution of particle sizes, changes in the spontaneous magnetization of the particle as function of temperature, or anisotropy effects.

Magnetic measurements of superparamagnetic particles may be used to determine the particle size distribution.[67] Particles with a given size are described by the Langevin function; integration of the Langevin function over a size distribution gives the total magnetization. Assuming a form for the distribution, the width and mean particle size can be determined from the magnetization as a function of field. This determination does not account for any interparticle interactions and can thus only be used in systems that can be treated as weakly interacting. Measurements of ferrofluids found that the type of particle size distribution could be linked to the preparation method. Grinding methods are best fit by the log-normal distribution, while Gaussian distributions fit fluids made with carbonyl processes and wet methods.[68] Other suggestions for distributions[69] and techniques to determine distributions have been suggested.[70−72]

F. Stoner−Wohlfarth Theory. Stoner−Wohlfarth (SW) theory was developed to describe the behavior of an assembly of single-domain, noninteracting particles with uniaxial anisotropy.[73] SW examines the effect of different types of anisotropy on the magnetic properties, including the coercivity and remanence, of fine particles. The most-used result evolving from SW theory concerns the behavior of the remanence:[74]

$$\frac{M^{DCD}(H)}{M(\infty)} = \left(1 - 2\frac{M^{IRM}(H)}{M(\infty)}\right) \quad (11a)$$

where M^{DCD} is the dc demagnetization remanence, M^{IRM} is the isothermal remanent magnetization, and $M(\infty) = M^{DCD}(H=\infty) = M^{IRM}(H=\infty)$. Most real materials do not strictly satisfy the noninteracting assumption, so the manner in which the data deviate from eq 11 is often used as a way of further investigating interactions.[75] Kelly et al.[76] suggested using the difference term, $\Delta M(H)$, where

$$\Delta M(H) = \frac{M^{DCD}(H)}{M(\infty)} - \left(1 - 2\frac{M^{IRM}(H)}{M(\infty)}\right) \quad (11b)$$

Positive values of $\Delta M(H)$ are attributed to the presence of stabilizing (ferromagnetic) interactions, while negative values are attributed to demagnetizing interactions. Both types of interactions may be observed in the same sample.[77,78] Equation 11b has the advantage of being applicable to strongly interacting systems, whereas direct calculation of the form of the magnetization for strongly interacting systems can be prohibitively difficult. Equation 11b has been especially important for application of magnetic recording media, in which strong interactions are present.[79−81]

Table 2. Magnetic Lengths for Ferromagnetic Materials Parametrized Using the Magnetic Lengths Given in Eqs 1

material	l_K/l_S	material	l_K/l_S
Ni	6.0	Co	2.0
Fe	7.1	$SmCo_5$	1.4

G. Theory of Holz and Scherer for Nanostructured Materials. SW is often applied to all types of systems but is really inappropriate when interactions between magnetic grains are dominant. Holz and Scherer[82] (HS) present a micromagnetic theory explicitly addressing the behavior of the ideal type-D nanostructure. Using the micromagnetic lengths given in eq 1, HS assume that crystallographic correlations within the space of the nanocrystals are on the order of the nanocrystallite size, d_{NC}. If the relationship $l_K \gg d_{NC} \gg l_S$ applies, crystal anisotropy plays no role in the magnetic properties, which are dominated instead by magnetostatic and exchange energies. Table 2 compares the length scales for the three elemental ferromagnets and a rare-earth alloy. In Ni and Fe, the ratios of the anisotropy to magnetostatic lengths are large compared to Co and $SmCo_5$, suggesting that the theory is more likely to apply to Ni and Fe than to Co or $SmCo_5$.

For nanostructured materials satisfying this assumption, 2D domain walls are represented by disclinations composed of a core (with dimension πl_s) having a (spin) polarization and a position. Magnetization changes occur not via the motion of domain walls but instead via disclination motion. Intrinsic motion of a disclination corresponds to reversal of the polarization, while extrinsic motion corresponds to changing core position. Sample coercivity is dominated by the extrinsic mechanism, which is dependent on the topology of the structure. The intrinsic coercivity is closely related to the micromagnetic description of magnetization reversal in small particles.

The HS model predicts a crossover between a $1/T$ and an exponential dependence of $H_c(T)$ at low temperatures. The two forms are interpreted as representing two different types of disclination entanglements. Both forms have been observed in NS Ni,[83] although the reason for the crossover between the two forms is not understood, nor is the physical origin of the two types

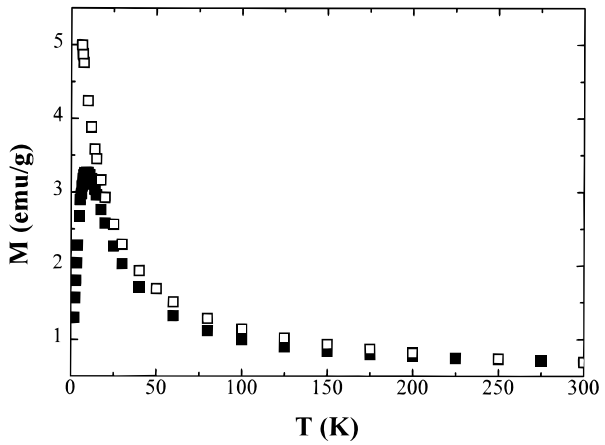

Figure 4. Magnetization as a function of temperature measured in the zero-field-cooled (solid symbols) and field-cooled (open symbols) cases for a nanocomposite consisting of cobalt particles in a polystyrene/triphenylphosphine matrix.

of entanglements. The HS model does not address time dependence at present.

H. Low-Temperature Ordering. Many nanostructures exhibit unusual low-temperature behavior suggestive of that observed in random or disordered magnetic systems. In most cases, the correlation between the magnetic behavior and the morphological origin of that behavior is not clear. Imry and Ma[84] showed that random fields, no matter how small, destroy long-range order in most magnetic systems. Randomness produces a range of different types of imperfectly ordered ground states.[85−89] These states have in common a cusp in the zero-field-cooled (ZFC) susceptibility and irreversibility between the ZFC and the field-cooled (FC) susceptibility.[90−94] Figure 4 shows the temperature dependence of the magnetization, $M(T)$, in a system consisting of Co nanoparticles randomly oriented in a polystyrene matrix.

The ZFC cusp is observed in spin glasses,[87] frozen ferrofluids with random anisotropy,[95−97] random anisotropy ferromagnets,[98] polymers containing magnetic components,[99,100] and superparamagnets, although the origin of the behavior is significantly different for each system. Superparamagnets below the blocking temperature are unable to thermally equilibrate, but no underlying phase transition is present.[101,102] In contrast, spin glasses[103] and random ferromagnets[99] exhibit a divergent nonlinear or singular susceptibility generally considered indicative of a phase transition. In each of these systems, the FC magnetization departs from the ZFC magnetization at some temperature (which may or may not be equal to the cusp temperature) and either reaches a plateau or monotonically increases below the cusp. In canonical spin glasses, the FC $M(T)$ departs from the ZFC $M(T)$ at or slightly above the cusp temperature and plateaus for temperatures below the cusp. In random anisotropy systems and frozen ferrofluids, the FC curve continues to rise monotonically with decreasing T below the cusp, as seen in Figure 4. The saturation or continuing rise of the FC curve below the cusp temperature is likely dependent on the magnitude of interactions and/or size effects.[104−106] Changing the mean particle diameter from 5 to 10 nm in an Fe_2O_3 sample with minimal interactions produces a plateau in M_{FC}/M_{ZFC}. Remanence measurements at temperatures below the cusp are also subject to time dependence.[107−110]

Frozen ferrofluids, in which the solvent freezes particles in random orientations, provides an ideal system for investigating this behavior, as exchange interactions are negligible and only the magnetic dipolar interaction is significant.[80,111] Interactions in ferrofluids can be easily varied (without modifying the particle distribution) by diluting the ferrofluid. An additional advantage is that the energy scale of the dipolar interaction depends directly on the magnitude of the dipole. Measuring dipolar interactions between individual spins requires an energy scale on the order of 10^{-3} K; since the ferromagnetic particles have on the order of 10^5 spins, the temperature scale for investigation of dipolar interactions is raised to tens of kelvin. Tuning of the interactions is limited by particle agglomeration at high concentrations.

III. Experimental Results

A. Fabrication Techniques. Synthesis and processing of metallic and ceramic nanostructured materials have been reviewed by several authors.[112,113] For the purposes of fabricating magnetic materials, the ideal synthesis technique provides control over particle or crystallite size, distribution of particle sizes, and interparticle spacing. Preparation-technique dependence has been observed, with materials having similar grain sizes but produced by different techniques exhibiting very different magnetic properties.

Chemical techniques are widely used to produce nanostructured materials due to their straightforward nature and the potential for producing large quantities of the final product. Realizable particles sizes range from nanometer to micron scale, with particle size controlled during synthesis by the competition between nucleation and growth. Disadvantages include the possible incorporation of intermediate products in the final product, and lack of fine control over the composition of alloy materials.

"Rieke Metals". In 1972, Rieke and co-workers reported a general approach for preparing highly reactive metal powders by reducing metal salts in ethereal or hydrocarbon solvents using alkali metals.[114−117] Since the initial report, several other reduction methods have been reported,[118−120] including metal−graphite compounds,[121] magnesium−anthracene complexes, and dissolved alkalides.[122,123]

Reductions are conveniently carried out with an alkali metal and a solvent whose boiling point exceeds the melting point of the alkali metal. The metal salt to be reduced must also be partially soluble in the solvent and the reductions:

$$MX_n + nK \rightarrow M^* + nKX \qquad (12)$$

are carried out under an argon atmosphere. M is the metal, X the halide, and K the alkali metal. An electron carrier may be used to produce alkali-metal ions during or prior to the reductive step. Variation of temperature allows control over reaction rates and, indirectly, particle size. This approach has been used to prepare Fe, Ni, and Co powders for magnetic studies but is broadly applicable to most other metals and alloys. Similar techniques have been used to produce semiconductor

particles.[124] Overall particle sizes range from a few nanometers to micron sized; however, transmission electron microscopy has shown that larger particles are generally type-D nanostructures, with features on the scale of tens of nanometers.

Borohydride Reductions. Borohydride reduction of transition metals has been an important synthetic technique for producing ultrafine particles.[125] Klabunde, Sorensen, and Hadjipanayis have used borohydride reduction to fabricate elemental particles (Fe[126] and Co[127]), as well as binary and ternary materials.[128−130] Alloy powders made via borohydride reduction tend to be amorphous in the as-synthesized state[131] and must be heat treated to achieve crystallinity. As with the Rieke process, synthesis products are highly dependent on reaction conditions, such a whether the reaction medium is aqueous or nonaqueous.[132] Particles produced by this method range in size from 2 to 100 nm and are of type A or type B, depending on postsynthesis treatment.

Vapor Trapping. Metal vapor deposition involves the evaporation of a metal in the presence of a solvent.[133,134] A modification of this process has been used to deposit iron particles on a cold (77 K) solvent.[135] Adsorption of a surfactant limits particle size by impeding growth. Codeposition of immiscible metals (such as Fe/Li[136,137]) can be used to form type-B particles. Lithium coatings successfully protect iron particles from oxidation. The Fe core is approximately 20 nm in diameter but is composed of smaller iron grains of 3−4 nm diameter due to the incorporation of solvent fragments. Controlled atmosphere annealing allows control over the growth of crystalline Fe regions via phase separation.

Sonochemistry. In sonochemistry, acoustic cavitation at high frequencies (kHz−MHz) causes bubbles in liquids to nucleate, grow, and collapse. Using high-energy excitation, localized areas can reach temperatures up to 5000 °C, with pressures of hundreds of atmospheres over a few microseconds. Large temperature gradients (up to 10^{10} K/s) assist in the production of metastable phases, such as pure amorphous iron.[138] Like chemical reduction, sonochemistry can produce particles with very highly reactive surfaces. Sonochemistry can be used to produce large volumes of material and is thus an attractive technique for industrial application.[139,140] In addition to type-A and type-B particles, ultrasound has also been used to fabricate type-C metal/polymer nanocomposites.[141]

Molecular Self-Assembly. Fabrication via molecular self-assembly is increasingly used to produce materials with highly uniform morphologies. Amphiphiles—a hydrophobic acyl chain and a hydrophilic phosphate group on a backbone—offer a versatile approach for forming structures ranging from spheres to cylinders.[142−145] One of the most popularly used techniques taking advantage of molecular self assembly is the fabrication of particles via inversed micelles.[146−149] Particles formed by this technique tend to be smaller (2−10 nm) and range from superparamagnetic to ferromagnetic at larger sizes. The surfactant molecules help prevent unwanted particle growth and may also protect particles from oxidation. This technique has the advantage of keeping the particles separated during synthesis and providing passivation.

Evaporation/Condensation and Evaporation/Condensation/Compaction. The combination of evaporation/condensation with optional compaction can be used to produce all four types of morphologies. In the evaporation/condensation step, a metal is evaporated in the presence of an inert gas. Collisions between the vaporized metal and the inert gas atoms form clusters that are then collected on a coldfinger. Cluster size is determined by the inert-gas pressure. Fabrication is performed in a high-vacuum chamber to reduce oxidation, although this advantage may be lost if the particles are exposed to air upon removal from the chamber. Particles may be purposely passivated by introducing a known quantity of oxygen-containing gas after deposition. As-fabricated particles are generally type A, with passivation used to produce type-B particles. Type-C nanocomposite systems can be produced by sandwiching particles in situ between thin films of a protective metal. Single element metals[150,151] and ceramics,[152,153] as well as alloys[154] have been made using this technique.

Type-D material can be produced via high-pressure compaction of evaporated/condensed material at ambient or high temperatures. A primary advantage of in situ compaction compared to ex situ compaction is the reduction of grain-boundary oxidation in the nanostructured material. An additional problem in any type of material requiring particle compaction is reduced porosity due to incomplete consolidation. Achieving densities of up to 99% may require high temperatures during consolidation, which can cause undesired grain growth.

Sputtering. Many of the initial investigations of size effects in magnetism were performed using multilayered materials.[155] Sputtering offers control of layer thicknesses down to fractions of a nanometer and can be used to make metallic or insulating samples. Sputtering is often used to fabricate nanocomposite (type C) materials in one of two ways. For materials with low mutual solubility, cosputtering produces relatively monodisperse magnetic particles in a matrix. For more soluble materials, the nanocomposite structure can also be achieved by sputtering multilayers thin enough to be discontinuous. Most sputtered nanocomposites consist of magnetic particles embedded in a nonmagnetoactive matrix. The length over which different particles are correlated depends on the volume fraction of the different phases. At percolation, particles form a continuous path through the sample and the magnetic properties begin to approach those of the bulk. As with in situ consolidation, the high-vacuum conditions under which sputtering is performed reduce contamination at the magnetic particle/matrix boundaries. If materials can be selected such that the magnetic and the nonmagnetic component are immiscible, annealing of the sputtered samples can be used to tune the grain size continuously over a relatively broad range.[156,157]

Mechanical Alloying. Mechanical alloying—also called ball milling—has been used to fabricate type-C and type-D materials.[158−160] Type-C materials are most often formed when the components being processed do not readily form alloys, while Type-D materials result from the decomposition of ordered alloys or the formation of new phases during processing. The nanostructure is obtained by repeated mechanical deformation and alloying as the powder is vigorously shaken in a vial containing a number of milling balls. Mechanical

alloying has the advantage of being able to produce large quantities of material and is already a commercial technology; however, the monodispersity of the magnetic components and the uniformity of their distribution throughout the matrix cannot be easily controlled. The nonequilibrium character of the process, however, offers the ability to make metastable nanocomposites that may not be achievable via other techniques. Mechanical alloying is often used to amorphize a material for subsequent partial recrystallization. Production of a continuous solid requires high-temperature consolidation, which can cause grain boundary oxidation, grain growth, phase formation, and increased porosity. Although mechanical alloying has been considered a "dirty" fabrication technique in the past, the availability of tungsten carbide components and use of inert atmosphere and/or high-vacuum processes produce samples with acceptably low impurity concentrations.

Carbon Arc. The Kretschmer technique is often used for the production of carbon fullerenes and has been adapted to the fabrication of fine particles.[161−163] A hole is drilled in a carbon rod and filled with the desired powder, and the assembly used as an electrode. This technique produces type-B particles consisting of a metal or oxide particle surrounded by a carbon shell, or type-A carbon-alloy particles. The ability of the carbon shell to protect metal particles from corrosion makes this technique attractive for the fabrication of oxygen-sensitive rare-earth-based materials.

Partial Recrystallization of Amorphous Materials. Type-D materials may be fabricated through partial recrystallization. The amorphous precursor is frequently made by a fast quench from the melt using a technique such as melt-spinning. This technique is highly useful for the production of two-phase materials in which a hard magnetic phase is coupled through a soft phase. Starting materials consist of 3−5 element alloys, with subsequent heating producing small crystallites (often of a subphase) in an amorphous matrix.[164−166] This technique has minimal interface contamination and, unlike powder techniques, can produce porosity-free samples. Variation of the annealing conditions allows control over grain sizes, and the technique can produce large quantities of material.[167]

B. Experimental Results. *1. Ultrafine Particle Systems.* The production of isolated metallic magnetic particles is difficult, as the large surface areas are easily oxidized or otherwise subject to corrosion. Controlled passivation is possible but often introduces interactions between the magnetic and the passivating materials. Most attempts to produce ideal type-A systems are made by measuring the particles in the form of a ferrofluid or microemulsion to maintain particle separation while only minimally modifying the particle surface. Oxide particles have the advantage of not being as oxidation sensitive and are also in high demand for magnetic recording applications. Many oxide particles have significant shape anisotropy, which allows the particle size to be much larger without becoming multidomain.

The majority of production techniques produce spherical particles. For catalysis, particle shape has generally been of little consequence; however, the presence of shape anisotropy can significantly enhance the magnetic properties. A recent demonstration of the production of metallic particles with shape anisotropy is the work of Gibson and Putzer,[168] who demonstrated the synthesis of single-crystal hexagonal cobalt platelets of diameter 150 nm and thickness 15 nm using ultrasonic-assisted chemical reduction. The shape anisotropy is perpendicular to the crystalline anisotropy direction. Lorenz microscopy indicates that the magnetic moment lies in the basal plane of the hexagonal platelets, in contrast to bulk cobalt where the moment lies along the *c* axis.

The evaporation/condensation technique has been used to produce Co,[149,169,170] FeCr,[171,172] and Fe,[171,172] all of which should theoretically be type-A particles; however, passivation is generally required for measurement of these materials outside the vacuum chamber. These particles are discussed further in the sections on Type-B materials.[130]

Important applications in ferrofluids, magnetic imaging and magnetic recording rely on oxides, which are primarily ferrimagnetic and antiferromagnetic.[173] Commonly used particulate media are dispersions of γ-Fe_2O_3,[57,174] cobalt-modified γ-Fe_2O_3,[52,175−177] CrO_2,[176] and barium ferrites.[178] Shape anisotropy relaxes critical particle size limits, so that needle-like particles with lengths up to 10s - 100s of microns remain single domain. Oxide particle studies focus on the effect of doping[179] on interactions, commonly in ferrites doped with Mn,[180,181] Sr,[182] Sr−Zn,[183] Ba,[180] Ba−Co,[184] Zn,[185] and Co.[52,177−179]

Ferrofluids. The surfactant coating on a magnetic particle opposes clustering due to steric repulsion; however, the surfactant may also affect the uniformity or magnitude of the magnetization due to quenching of surface moments. Differences between the average particle size determined by microscopy and that determined from magnetization measurements suggest the existence of a magnetically dead layer at the surface. Applications of ferrofluids have been recently reviewed by Zahn and Shenton.[186]

Ferrofluids are ideal systems in which to investigate low-temperature ordering phenomena. Frozen ferrofluid systems exhibit a peak in the ZFC magnetization and irreversibility between the FC and ZFC magnetizations. In systems with very small particles, the phenomena is likely due to superparamagnetism; however, if the carrier fluid is frozen and the particles have uniaxial anisotropy, the random orientations of the particles on freezing can induce a random anisotropy. The low-temperature behavior of frozen ferrofluids exhibits many similarities to random anisotropy and spin glass systems.[97,187−190] Theoretical work has thus far not been able to explain the observed experimental differences between the different types of ordering phenomena.[191]

2. Core-Shell Particles. The majority of realizable samples fall into the intermediate (type-B and type-C) categories. Magnetic effects in these systems are due to a combination of size, as in isolated ultrafine particle systems, and interaction, as in type-D nanostructured materials. Type-A materials often inadvertently become core-shell particles due to oxidation. Although oxide shells often increase coercivity and remanence,[148,192] size effects can be obscured. A theoretical understanding of surface anisotropy is necessary to determine how to separate these two phenomena.[193−196]

Klabunde, Sorensen, and Hadjipanayis have investigated the core-shell morphology in both elemental and alloy particles.[197−199] Observed particle size dependence is usually due to the shell becoming a greater fraction of the particle volume as the total particle size decreases. A reduction in saturation magnetization is often reported in type-B core-shell particles, usually due to the loss of net moment in the antiferromagnetic or ferrimagnetic oxide shell. Theoretical calculations suggest that effects are most dominant when the axes of the surface anisotropy and the bulk anisotropy are not collinear.[200]

Purposely oxide-passivated Co,[201] CoFe,[201−203] and Ni[204,205] particles are used to study unidirectional anisotropy induced by exchange coupling. Unidirectional anisotropy is identified by a shift of the hysteresis loop toward negative fields following cooling in a large field. The oxide shells generally have small (on the order of a few nanometers) crystallites, which allows them to remain undetected in most X-ray diffraction measurements. An interesting observation is that the effects of the unidirectional anisotropy often disappear at a temperature (150 K in Co/CoO) that can be identified as the reduced Néel temperature for very small grains. Intentional coating with non-oxide layers (such as Pd[206,207]) or passivation by nitrogen[208] can also increase the coercivity. Coatings can be introduced during chemical reduction and used as surfactants to control particle size.[209]

3. Nanocomposites. The embedding of magnetic particles in a matrix began as an offshoot of thin-film and multilayer studies. Ferromagnetic particles in a nonmagnetic host ("granular ferromagnets") exhibit giant magnetoresistance phenomena and may have applications in magnetic recording heads. The electrically insulating or conductive nature of the matrix can also affect the magnetic properties of the nanocomposite. As with core-shell particles, nanocomposites isolate and protect the magnetic components at the cost of possible interactions between surface spins and the matrix. Nanocomposites also assist in preventing agglomeration of magnetic particles by fixing them rigidly within the matrix, which may provide a way of tuning interactions over a broader range possible than in ferrofluids.

Magnetic properties of nanocomposites are often measured as a function of volume fraction of the magnetic component, with the maximum coercivity occurring at volume fractions below the percolation concentration. Percolation encourages the formation of magnetic closure loops, which decrease the coercivity. The most-investigated systems are based on matrixes of Al_2O_3 (with particles of Co,[210] FeNi,[211,212] FeCo,[214,215] Ni,[219,220] and Fe[213−215]) and SiO_2 (with particles of Fe[214,215] and Ni[216,217]). SiO_2 can form impurity phases with many of the magnetic materials, suggesting that Al_2O_3 is a superior matrix material.[214,215] Immiscible systems, such as Fe/Cu[218,219] have been fabricated by many techniques. Sol−gel processes have also produced Fe/SiO_2[220] and FeNi/SiO_2.[221] Systems made using sputtering usually show a behavior similar to that of those made using mechanical alloying.[222] Reaction alloying, in which mechanical alloying is used to produce a chemical reduction, has been used to make nanocomposites such as Fe/ZnO,[223,224] SmCo/CaO,[225] and Fe_3O_4/Cu.[226]

In some special cases, metallurgical considerations allow the production of small, discrete grains of a magnetic material in a nonmagnetic material under very specific annealing conditions. One example is CoAl β-phase alloys with aluminum concentrations between 25 and 40%.[227] Under appropriate heat treating, single-domain lath or platelike particles of cobalt form in a CoAl matrix. The platelets orient themselves preferentially along the matrix crystallographic axes, imposing some overall orientational order on the assembly and producing coercivities up to 2 kOe. Although the number of systems that can be produced using this technique is limited, the materials have clean interfaces and low porosity.

Intercalation techniques produce sheets of magnetic material, with coupling between sheets responsible for cooperative behavior.[228] These materials offer a layered geometry much like their sputtered multilayered cousins, but with fabrication control at the molecular level. Continued improvements will allow more sensitive probes of the effect of dimensionality on magnetic properties.

One of the most interesting nanocomposite subclasses is the self-stabilized magnetic colloid: magnetic particles suspended in a polymeric matrix. Polymer/magnetic metal nanocomposites have potential applications in electromagnetic shielding and as hosts for highly reactive particles. As many ultrafine particles are pyrophoric, a polymeric matrix could ease transportation and storage of the particles with the possibility of future retrieval. As with all intermediate types, the polymer matrix separates the particles but may also provide interparticle magnetic coupling. Effects on the polymer structure due to the presence of magnetic particles is also possible. In composites with micron-size filler metals, the main polymeric chain length decreases and a more rigid network in the boundary layer surrounding the particle is formed. The ends of the main-chain polymers are anchored at the filler surface, reducing the molecular mobility of the polymer even quite a distance from the filler.[229] The effect of smaller particles—especially on the structural relaxation of polymers—remains to be studied. In macroscopic composites, the polymeric matrix is involved in the magnetic behavior due to the collective states of the π-electrons (magnetic solitons) in the presence of the ferromagnetic metallic clusters.[230] At low metal concentrations, the magnetic susceptibility exhibits a cusp at the glass transition temperature of the host, indicating coupling between the polymer degrees of freedom and the magnetic behavior. As the metal concentration increases, particle−particle interactions dominate particle−matrix interactions. A number of groups have synthesized nanoscale magnetic particles (Fe,[231,232] Co,[233,234] maghemite,[13,235,236] and Fe_3O_4[237]) within a polymer matrix. On the other end of the size scale, macroscopic composites of 10−100 μm sized transition metal powders[238,239] and ferrites[240] have been fabricated to study modifications of electrical and magnetic properties.

Ziolo and co-workers[13,238] used ion-exchange resins to fabricate iron oxides and lead iodides. Fe_2O_3 in ion exchange resins produces an optically transparent magnetic material. Oxide particles range from 5 to 25 nm in diameter. Smaller particle nanocomposites are

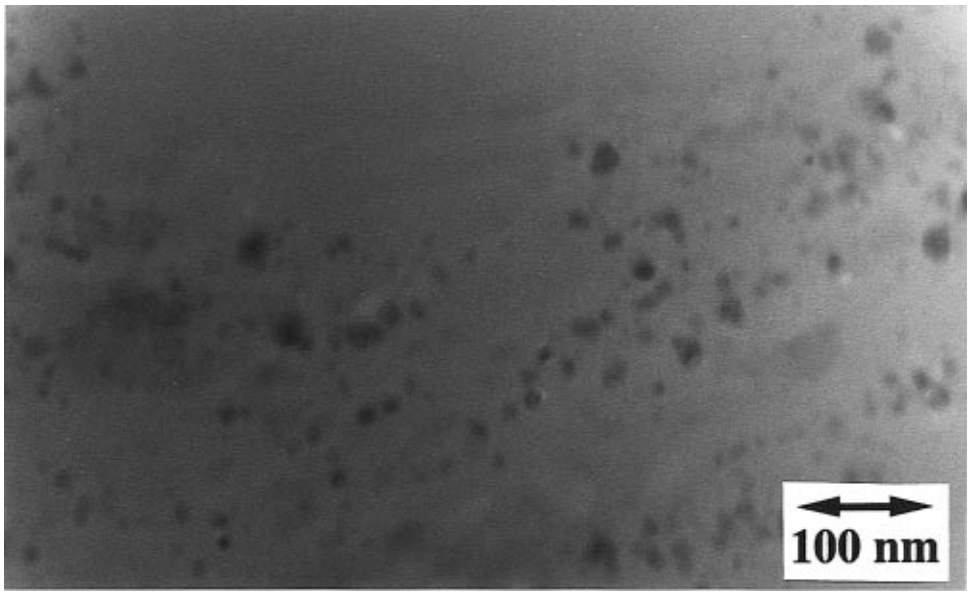

Figure 5. TEM bright-field image of a cobalt/polymer nanocomposite after annealing. Nanodiffraction shows no evidence of crystallinity in the cobalt particles.

superparamagnetic, while larger particle nanocomposites (25 nm) are ferromagnetic at room temperature.

The Rieke technique was first used to bind active metal particles to a polymer matrix in 1990[241,242] and has recently been used to produce cobalt particles in a polystyrene-based polymer.[237] The degree of polymer cross-linking and solvent choice produce significant variations in the magnetic properties, with the as-synthesized systems ranging from superparamagnetic to ferromagnetic. Solvent selection has been shown to affect particle size in similar syntheses.[126] Figure 5 shows a transmission electron micrograph of a polymer nanocomposite with approximately 20 nm spherical cobalt particles.[236] Nanobeam diffraction (spot size ~ 5 nm) shows no evidence of crystallinity in the cobalt particles. Annealing increases H_c and M_r/M_s, with values as high as 600 Oe and 0.42, respectively. The ZFC M(T) exhibits a cusp at temperatures ranging from 5 to 20 K, depending on sample parameters. An example of this behavior was shown in Figure 3. The origin of this behavior is likely due to the random orientations of the uniaxial anisotropy, size distribution, and interparticle distance distribution.

Highly monodisperse cobalt nanoparticles (diameter 1 nm) in a polymer matrix have been made by sputtering.[236] Even at this small size, the clusters have a bulklike magnetization at low temperature, and the Curie temperature remains above room temperature. Roughly half the atoms on the surface of the cobalt clusters are in contact with polymer; the retention of bulklike properties suggests minimal interaction with the matrix, as also observed in Co/Cu granular ferromagnets.[243,244] Electrical percolation occurs around a metal volume fraction of 22%. Low cobalt volume fraction samples are superparamagnetic, while larger volume fractions become ferromagnetic. Magnetic nanocomposites have also used zeolite hosts, although earlier zeolite templates were limited to smaller particle sizes.[245]

4. Nanostructured Materials. The Holz−Scherer theory describes an ideal single component type-D material. The volume fraction of atoms in grain boundaries can be as large as 50% for 5 nm grains, decreasing to 5% for 10 nm grains, and 3% for 100 nm grains. The Type-D group also includes materials in which nanocrystallites are precipitated from an initially amorphous matrix.

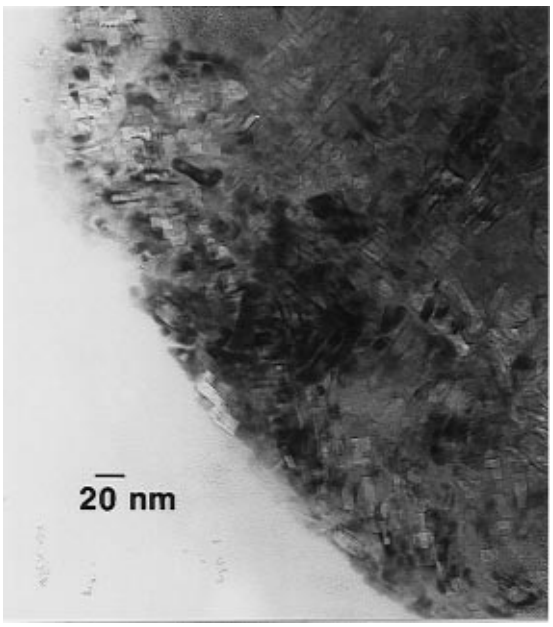

Figure 6. TEM bright field image of a Ni/Ni_3C nanostructure made by chemical reduction.

Metallic particles grown using the Rieke technique have nanostructure on the scale of 5−50 nm. Figure 6 shows a bright-field transmission electron micrograph of a Ni/Ni_3C nanocomposite annealed at 250 °C for 2 h.[246] X-ray diffraction indicates that the as-synthesized particles have crystallite sizes less than 5 nm. The formation of Ni_3C during annealing suggests that solvent fragments are incorporated into the material during synthesis. Incompletely crystallized samples are likely composed of small Ni crystallites in an amorphous matrix of Ni−C. The unique nanostructure produces coercivities up to 2 orders of magnitude larger than polycrystalline nickel. Remanence ratios approaching 0.5 suggest minimal net coupling between the magnetic components. Maximum coercivities occur with Ni crys-

tallite sizes of approximately 20 nm. Ni and Ni_3C have also been made by vapor deposition, although no magnetic properties were reported.[247]

Measurements of nanostructured nickel formed by in situ compaction of evaporated Ni powders were described by Schaefer et al.[84] Initial reports suggested that the interphase had a Curie temperature and moment per atom between that of the crystalline[248] and amorphous forms. Subsequent reports[249] suggest that these early conclusions were due to oxide contamination of the interfaces and surfaces. The high-purity material showed no decrease in the bulk magnetization, and the Curie temperature was not reported. Measurements of nanostructured Fe made by evaporation/condensation/compaction show that M_s in samples with 6 nm grain size decreases by 40% from the bulk value.[250] Nanostructured iron and nickel have been made by mechanical alloying, although interpretation of the results is complicated by the introduction of impurities during the milling.[251,252] In addition to grain boundary contamination, determination of the saturation magnetization may also be affected by voids in compacted materials.[253] Conclusions about the fundamental properties of materials in their nanostructured forms require very careful sample characterization.

The fabrication of exchange-coupled two-phase nanostructures has been of interest for application to both permanent magnet and soft magnetic materials.[254,255] Annealing of amorphous FeCuNbSiB produces nanosized Fe_2B grains in an amorphous matrix, with grain sizes of 10−12 nm providing optimal soft magnetic properties.[256] The discovery of remanence enhancement in isotropic fine-grained materials has generated much interest in exchange coupling between magnetically hard and soft phases. The first experimental observations were in $Nd_2Fe_{14}B$ compounds, which exhibited remanence ratios up to 0.9.[169,257−263] Subsequent studies focused on $Sm(Fe,X)_{12}$,[264] $(Sm,Zr)Fe_3$,[265] $Sm_2Fe_{17}N_x$,[266−268] FeZr,[269] and CoNbB.[270] Similar structures optimized for high remanence and coercivity have been formed by in the SmCo family by mechanical alloying,[225,271−273] and in sputtered SmCo/CoFe multilayers.[274] In 1991, Kneller and Hawig[275] suggested that anisotropy could be transmitted across hard and soft magnetic phases via exchange coupling. Analytical calculations[276] and simulations[277−279] suggest that maximum remanence and coercivity occur when the soft phase is on the order of the domain wall width of the hard phase, which translates to grain sizes of 10−30 nm. The effect of chemical additions to control grain size has also been investigated.[280]

IV. Promising Developments

One of the most significant roles for nanostructures in terms of magnetism is investigating the transition between polycrystalline materials and individual atoms or small clusters. Atomic-level magnetization is primarily done in ultrahigh-vacuum chambers on monolayers or bilayers of a material on a specific substrate. Correlation between these experiments and macroscopic measurements of nanostructured material is essential. As an example, experimental macroscopic measurements of nanostructured nickel[252] suggest that the interphase magnetization is no different than that of the bulk. A UHV experiment,[281] in which the atomic and magnetization densities in a single nickel twist grain boundary were measured, found that the magnetic moment per atom was increased between 18% and 52% in the boundary. The reduced density of the interphase is predicted to produce an overall enhancement of only about 10%, which means that morphologically and chemically well-controlled samples will be essential to testing this prediction.

The fabrication of materials within controlled geometries, such as track-etched membranes and nanochannel glasses, will improve the ability to produce monodisperse, well-separated particle systems with minimal interactions.[282−284] Electrodeposition into these materials has already been used to make multilayered wires.[285]

Finally, improving our ability to fabricate magnetic structures for applications requires input from a broad range of disciplines. Increased collaboration, the application of highly local measurement techniques (such as neutron scattering), and better dialogue between members of the different materials communities will greatly advance our ability to fabricate and understand nanostructured materials.

Acknowledgment. The authors thank Gary Krichau for the micrograph in Figure 6 and Richard L. Schalek for the micrograph shown in Figure 5. Support from the National Science Foundation (OSR9553350) is gratefully acknowledged.

References

(1) Eastman, Jeff; Siegel, Richard W. *Res. Dev.* **1989**, *31*, 56.
(2) Siegel, R. W. *Nanostruct. Mater.* **1993**, *3*, 1.
(3) Gleiter, H. *Prog. Mater. Sci.* **1989**, *33*, 223.
(4) Gryaznov, V. G.; Trusov, L. I. *Prog. Mater. Sci.* **1993**, *37*, 289.
(5) Dormann, J.; Fiorani, D. *Magnetic Properties of Fine Particles;* North-Holland: Amsterdam, 1992.
(6) Kear, B. H.; Cross, L. E.; Keem, J. E.; Siegel, R. W.; Spaepen, F.; Taylor, K. C.; Thomas, E. L.; Ru, K.-N. *Research Opportunities for Materials with Ultrafine Microstructures Vol NMAB-454*; National Academy: Washington DC, 1989.
(7) Suryanarayana, C. *Int. Mater. Rev.* **1995**, *40*, 41.
(8) Shull, R. D. *Report on the First NIST Workshop on Nanostructured Materials*; National Institute of Standards and Technology: Washington DC, 1994.
(9) Gleiter, H. *Nanostruct. Mater.* **1992**, *1*, 1.
(10) Gunther, L. *Phys. World* **1990**, *2*, 28.
(11) Shull, Robert D. *IEEE Trans. Magn.* **1993** *29*, 2614.
(12) Shull, R. D.; McMichael, R. D.; Schwartendruber, L. J.; Bennett, L. H. *Proceedings of the 7th International Cryocoolers Conf.* (*Nov 1992*); Ludwigsen, J., Stoyanoff, M., Eds.
(13) Ziolo, R. F.; Giannelis, E. P.; Weinstein, B.; O'Horo, M. P.; Ganguly, B. N.; Mehrotra, V.; Russell, M. W.; Huffman, D. R. *Science* **1992**, *257*, 219.
(14) Anton, I.; et al. *J. Magn. Magn. Mater.* **1990**, *85*, 219.
(15) Raj, K.; Moskowitz, B.; Casciari, R. *J. Magn. Magn. Mat*er. **1995**, *149*, 174.
(16) Odenbach, Stefan *Adv. Colloid Interface Sci.* **1993**, *46*, 263.
(17) Scholten, P. C. *J. Magn. Magn. Mater.* **1995**, *57*, 149.
(18) Wagner, W.; Van Swygenhoven, H.; Höfler, H. J.; Wiedenmann, A. *Nanostruct. Mater.* **1995**, *6*, 929.
(19) Kronmüller, H. *Moderne Problerme der Metalphysik II*, edited by Alfred Seeger; Springer: Berlin, 1966.
(20) Cullity, B. D. *Introduction to Magnetic Materials*, Addison-Wesley Publishing Company: Reading, MA, 1972.
(21) Meiklejohn, W. H.; Bean, C. P. *Phys. Rev.* **1956**, *102*, 1413.
(22) Meiklejohn, W. H.; Bean, C. P. *Phys. Rev.* **1957**, *105*, 904.
(23) Meiklejohn, W. H.; *J. Appl. Phys.* **1962**, *33*, 1328.
(24) Bean, C. P.; Livingston, J. D. *J. Appl. Phys.* **1959**, *30*, 120S.
(25) Bean, C. P. In *Structure and Properties of Thin Films*; Neugebauer, C. A., Newkirk, J. B., Vermilyea, D. A., Eds.; Wiley: New York, 1959; p 331.
(26) Jacobs, I. S.; Bean, C. P. Fine Particles, Thin Films and Exchange Anisotropy (Effects of Finite Dimensions and Interfaces on the Basic Properties of Ferromagnets). In: *Magnetism*; Rado, G. T., Suhl, H., Eds.; Academic Press: New York, 1963; Vol. III, p 271.
(27) Brown, Jr., W. F. *Micromagnetics*; Wiley-Interscience: New York, 1963.

(28) Wohlfarth, E. P. In *Magnetism*; Rado, G. T., Suhl, H., Eds.; Academic Press: New York, 1963; Vol. III, p 351.
(29) Kneller, E. In *Magnetism and Metallurgy*; Berkowitz, A., Kneller, E.; Academic Press: New York, 1969; Vol. 1, p 365−371.
(30) Stoner, E. C.; Wohlfarth, E. P. *Proc. Phys. Soc.* **1948**, *240*, 599.
(31) Néel, L. *C. R. Acad. Sci.* **1947**, *224*, 1488 (English translation: Kurti, N. *Selected Works of Louis Néel*; Gordon and Break Science Publishers: New York, 1988).
(32) Frenkel, J.; Dorfman, J. *Nature* **1930**, *126*, 274.
(33) Kittel, C. *Phys. Rev.* **1946**, *70*, 965.
(34) Néel, L. *J. Phys. Rad.* **1951**, *12*, 339.
(35) Néel, L. *Ann. Geophys.* **1949**, *5*, 99.
(36) Brown, W. F. *J. Appl. Phys.* **1959**, *30*, 130S.
(37) Kneller, E. *Proceedings of the International Conference of Magnetism*; Physical Society of London, 1965.
(38) Brown Jr., W. F. *Phys. Rev.* **1963**, *130*, 1677.
(39) Aharoni, A. *Phys. Rev.* **1963**, *177*, 1677.
(40) Dickson, D. P. E.; Reid, N. M. K.; Hunt, C.; William, H. D.; El-Hilo, M.; O'Grady, K. *J. Magn. Magn. Mater.* **1993**, *125*, 345.
(41) Xiao, Gang; Liou, S. H.; Levy, A.; Taylor J. N.; Chien, C. L. *Phys. Rev B* **1986**, *34*, 7573.
(42) Chantrell, R. W. *J. Magn. Magn. Mater.* **1991**, *95*, 365.
(43) Street, R.; McCormick, P. G.; Estrin, Y. *Proc. Int. Workshop Rare-Earth Magnets*; Kyoto, Japan, 1989.
(44) Aharoni, A. *J. Appl. Phys.* **1985**, *57*, 4702.
(45) El-Hilo, M.; O'Grady, K.; Chantrell, R. W. *J. Magn. Magn. Mater.* **1992**, *109*, L164.
(46) Lottis, D. K.; White, R. M.; Dahlberg, E. D. *Phys. Rev. Lett.* **1991**, *67*, 362.
(47) Chamberlin, R. V.; Holtzberg, F. *Phys. Rev. Lett.* **1991**, *67*, 1606.
(48) Chamberlin, R. V.; Haines, D. N. *Phys. Rev. Lett.* **1990**, *65*, 2197.
(49) Mayo, P. I.; O'Grady, K.; Chantrell, R. W.; Cambridge, J. A.; Saunders, I. L.; Yogi, T.; Howard, J. K. *J. Magn. Magn. Mater.* **1991**, *95*, 109.
(50) Wohlfarth, E. P. *J. Phys. F* **1983**, *14*, L155.
(51) de Witte, A. M.; O'Grady, K. *IEEE Trans. Magn.* **1990**, *26*, 1810.
(52) Zhong, X. P.; Wang, G. H.; Luo, H. L. *J. Magn. Magn. Mater.* **1993**, *120*, 190.
(53) Chantrell, R. W.; Fearon, M.; Wohlfarth, E. P. *Phys. Status Solidi* **1986**, *97*, 213.
(54) O'Grady, K.; Chantrell, R. W. *J. Magn. Magn. Mater.* **1986**, *54−57*, 757.
(55) El-Hilo, M.; Uren, S.; O'Grady, K.; Popplewell, J.; Chantrell, R. W. *IEEE Trans. Magn.* **1990**, *26*, 244.
(56) deWitte, A. M.; O'Grady, K.; Coverdale, G. N.; Chantrell, R. W. *J. Magn. Magn. Mater.* **1990**, *88*, 183.
(57) Oseroff, S. B.; Clark, D.; Schulz, S.; Shtrikman, S. *IEEE Trans. Magn.* **1986**, *21*, 1495.
(58) Uren, S.; Walker, M.; O'Grady, K.; Chantrell, R. W. *IEEE Trans. Magn.* **1988**, *20*, 1808.
(59) O'Grady, K.; Chantrell, R. W.; Popplewell, J.; Charles, S. W. *IEEE Trans. Magn.* **1981**, *17*, 2943.
(60) Chantrell, R. W.; Lyberatos, A.; El-Hilo M.; O'Grady, K. *J. Appl. Phys.* **1994**, *76*, 6407.
(61) Néel, L. *C. R. Acad. Sci.* **1949**, *228*, 664.
(62) Chantrell, R. W.; El-Hilo, M.; O'Grady, K. *IEEE Trans. Magn.* **1991**, *27*, 3570.
(63) Wohlfarth, E. P. *J. Phys. F: Met. Phys.* **1980**, *10*, L241.
(64) Heukelon, W.; Broeder, J. J.; Van Reijen, L. L. *J. Chim. Phys.* **1954**, *51*, 474.
(65) Becker, J. J. *Trans. Am. Inst. Mining Met. Petrol. Engrs.* **1957**, *209*, 59.
(66) Bean, C. P.; Jacobs, I. S. *J. Appl. Phys.* **1956**, *27*, 1448.
(67) Chantrell, R. W.; Popplewell, J.; Charles, S. W. *IEEE Trans. Magn.* **1978**, *14*, 975.
(68) O'Grady, K.; Bradbury, A. *J. Magn. Magn. Mater.* **1983**, *39*, 91.
(69) Mahmood, Sami H. *J. Magn. Magn. Mater.* **1993**, *118*, 359.
(70) Mørup, S.; Dumesic, J. A.; Topsøe, H. *Application of Mössbauer Spectroscopy*; Cohen, R. L., Ed.; Academic Press: New York, 1980; Vol. 2.
(71) Mørup, S.; *Mössbauer Spectroscopy Applied to Inorganic Chemistry*; Long, G. J., Ed.; Plenum Press: New York, 1984; Vol. 2.
(72) Mørup, S.; Topsøe, H.; Clausen, B. S. *Phys. Scr.* **1982**, *25*, 713.
(73) Stoner, E. C.; Wohlfarth, E. P. *Proc. Phys. Soc. A* **1948**, *240*, 599.
(74) Wohlfarth, E. P. *J. Appl. Phys.* **1958**, *29*, 595.
(75) Henkel, O. *Phys. Status Solidi* **1964**, *7*, 919.
(76) Kelly, P. E.; O'Grady, K.; Mayo, P. I.; Chantrell, R. W. *IEEE Trans. Magn.* **1989**, *25*, 3881.
(77) Mayo, P. I.; Erkkila, R. M.; Bradbury, A.; Chantrell, R. W. *IEEE Trans. Magn.* **1991**, *26*, 1894.
(78) Mayo, P. I.; Bradbury, A.; Chantrell, R. W. Kelly, P. E.; Jones, H. E.; Bissell P. R. *IEEE Trans. Magn.* **1990**, *26*, 228.
(79) O'Grady, K.; El-Hilo, M.; Chantrell, R. W. *IEEE Trans. Magn.* **1993**, *29*, 2608.
(80) Webb, B. C.; Schultz, S.; Oseroff, S. B. *J. Appl. Phys.* **1988**, *63*, 2923.
(81) Coverdale, G. N.; Chantrell, R. W.; O'Grady, K. *J. Magn. Magn. Mater.* **1990**, *83*, 442.
(82) Holz, A.; Scherer, C. *Phys. Rev B* **1994**, *50*, 6209.
(83) Schaefer, H.-E.; Kisker, H.; Kronmuller, H. Wurschum, R. *Nanostruct. Mater.* **1992**, *1*, 523.
(84) Imry, Y.; Ma, S.-K. *Phys. Rev Lett.* **1975**, *35*, 1399.
(85) Coey, J. M. D. *J. Appl. Phys.* **1978**, *49*, 1646.
(86) Binder, K.; Young, A. P. *Rev. Mod. Phys.* **1986**, *58*, 801.
(87) Chudnovsky, E. M.; Saslow, W. M.; Serota, R. A. *Phys. Rev. B* **1986**, *33*, 251.
(88) Chudnovsky, E. M. *J. Appl. Phys.* **1988**, *10*, 5770.
(89) Chudnovsky, E. M.; Serota, R. A. *Phys. Rev. B* **1982**, *26*, 2697.
(90) Mørup, S. *Europhys. Lett.* **1994**, *28*, 671.
(91) Aharony, A.; Pytte, E. *Phys. Rev. Lett.* **1980**, *45*, 1583.
(92) Zaluska-Kotur, M. A.; Cieplak, M. *Europhys. Lett.* **1993**, *23*, 85.
(93) Bouchard, J. P.; Zérah, P. G. *Phys. Rev.* B **1993**, *47*, 9095.
(94) Romano, S. *Phys. Rev. B* **1994**, *49*, 12287.
(95) Ayoub, N. Y.; Abdelal, R. Y.; Chantrell, R. W.; Popplewell, J.; O'Grady, K. *J. Magn. Magn. Mater.* **1989**, *79*, 81.
(96) Luo, W.; Nagel, S. R.; Rosenbaum, R. F.; Rosenzweig, R. E. *Phys. Rev. Lett.* **1991**, *67*, 2721.
(97) El-Hilo, M.; O'Grady, K.; Chantrell, R. W. *J. Magn. Magn. Mater.* **1992**, *114*, 307.
(98) Sellmyer, D. J.; Nafis, S. *Phys. Rev. Lett.* **1986**, *57*, 1173.
(99) Palacio, F.; Castro, C.; Lázaro, F. J.; Reyes, J. *J. Magn. Magn. Mater.* **1992**, *104−107*, 2101.
(100) Jarjayes, O.; Fries, P. H.; Bidan, G. *J. Magn. Magn. Mater.* **1994**, *137*, 205.
(101) Wohlfarth, E. P. *Phys. Lett.* **1979**, *70A*, 489.
(102) El-Hilo, M.; O'Grady, K.; Popplewell, J.; Chantrell, R. W.; Ayoub, N. *J. Phys.* **1989**, *C8*, 1835.
(103) Levy, L. P. *Phys. Rev. Lett.* **1988**, *38*, 4963.
(104) Tronc, E.; Prené, P.; Jolivet, J. P.; Fiorani, D.; Testa, A. M.; Cherkaoui, R.; Noguès; M.; Dormann, J. L. *Nanostruct. Mater.* **1995**, *6*, 945.
(105) Prené, P.; Tronc, E.; Jolivet, J.-P.; Livage, J.; Cherkaoui, R.; Noguès, M.; Formann, J.-L.; Fiorani, D. *IEEE Trans. Magn.* **1993**, *29*, 2658.
(106) Mørup, S.; Tronc, E. *Phys. Rev. Lett.* **1994**, *72*, 3278.
(107) Dormann, J. L.; Fiorani, D.; Tholence, J. L.; Sella, C. *J. Magn. Magn. Mater.* **1983**, *35*, 117.
(108) El-Hilo, M.; O'Grady, K. *IEEE Trans. Magn.* **1990**, *26*, 1807.
(109) Aharoni A.; Wohlfarth, E. P. *J. Appl. Phys.* **1984**, *55*, 1664.
(110) El-Hilo, M.; O'Grady, K.; Popplewell, J. *J. Appl. Phys.* **1991**, *69*, 5133.
(111) El-Hilo, M.; O'Grady, K. and Chantrell, R. W. *J. Magn. Magn. Mater.* **1992**, *114*, 295.
(112) Siegel, R. W. *Mechanical Properties and Deformation Behavior of Materials Having Ultra-Fine Microstructures*; Nastasi, M., et al., Eds.; Kluwer Academic Publishers: Dordrecht, The Netherlands, 1993.
(113) Andres, R. P.; Averback, R. S.; Brown, W. L.; Brus, L. E.; Goddard III, W. A.; Kaldor, A.; Louie, S. G.; Moskovits, M.; Peercy, P. S.; Riley, S. J.; Siegel, R. W.; Spaepen F.; Wang, Y. *J. Mater. Res.* **1989**, *4*, 704.
(114) Rieke, R. D. *Top. Curr. Chem.* **1975**, *59*, 1.
(115) Rieke, R. D. *Acc. Chem. Res.* **1977**, *10*, 301.
(116) Burns, T. P.; Rieke, R. D. *J. Org. Chem.* **1987**, *52*, 3674.
(117) Rieke, Reuben D. *Crit. Rev. Surf. Chem.* **1991**, *1*, 131.
(118) Csuk, R.; Glanzer, B. L.; Furstner, A. *Adv. Organomet. Chem.* **1988**, *28*, 85.
(119) Savoia, D.; Tombini, C.; Umani-Ronchi, A. *Pure Appl. Chem.* **1986**, *57*, 1977.
(120) Bogdanovic, B. *Acc. Chem. Res.* **1988**, *21*, 261.
(121) Marceau, P.; Gautreau, L.; Beguin, F. *J. Organomet. Chem.* **1991**, *403*, 21.
(122) Tsai, K. L.; Dye, J. *Faraday Discuss. Chem. Soc.* **1991**, *92*, 45.
(123) Tsai, K.-L.; Dye, J. *J. Am. Chem. Soc.* **1991**, *113*, 1650.
(124) Kher, S. S.; Wells, R. L. *Chem. Mater.* **1994**, *6*, 2056.
(125) van Wonterghen, J.; Mørup, S.; Koch, C. J. W.; Charles, S. W.; Wells, S. *Nature* **1986**, *322*, 622.
(126) Glavee, G. N.; Klabunde, K. J.; Sorensen, C.; Hadjipanayis, G. C. *Inorg. Chem.* **1995**, *34*, 28.
(127) Glavee, G. N.; Klabunde, K. J.; Sorensen, C. M.; Hadjipanayis, G. C. *Inorg. Chem.* **1993**, *32*, 474.
(128) Glavee, G. N.; Klabunde, K. J.; Sorensen, C. M.; Hadjipanayis, G. C.; Tang, Z. X.; Yiping, L. *Nanostruct. Mater.* **1993**, *3*, 391.
(129) Yiping, L.; Hadjipanayis, G. C.; Sorensen, C. M.; Klabunde, K. J. *J. Appl. Phys.* **1991**, *69*, 5141.
(130) Yiping, L.; Tang, Z. X.; Hadjipanayis, G. C.; Sorensen, C. M.; Klabunde, K. J. *IEEE Trans. Magn.* **1993**, *26*, 2646.
(131) Saida, J.; Ghafari, M.; Inoue A.; Masumoto, T. *J. Non-Cryst. Solids* **1993**, *156−158*, 547.
(132) Glavee, G. N.; Klabunde, K. J.; Sorensen, C. M.; Hadjipanayis, G. C. *Langmuir* **1992**, *8*, 771.
(133) Klabunde, K. J.; Timms, P. L.; Skell, P. S.; Ittel, S. *Inorg. Synth.* **1979**, *19*, 59.
(134) Groshens, T. J.; Klabunde, K. J. *Experimental Organometallic Chemistry*; Wayda, A. L., Darensbourg, M. Y., Eds.; ACS Symposium Series, No 357; American Chemical Society: Washington DC, 1987.
(135) Kernizan, C. F.; Klabunde, K. J.; Sorensen, C. M.; Hadjipanayis, G. C. *Chem. Mater.* **1990**, *2*, 70.

(136) Glavee, G. N.; Kernizan, C. F.; Klabunde, K. J.; Sorensen, C. M.; Hadjipanayis, G. C. *Chem. Mater.* **1991**, *3*, 967.
(137) Glavee, G. N.; Eason, K.; Klabunde, K. J.; Sorensen, C. M.; Hadjipanayis, G. C. *Chem. Mater.* **1992**, *4*, 1360.
(138) Grinstaff, M. W.; Salamon, M. B.; Suslick, K. S. *Phys. Rev. B* **1993**, *48*, 269.
(139) Suslick, K. S. *Science* **1990**, *247*, 1440.
(140) Suslick, K. S. *MRS Bull.* **1995**, *4*, 29.
(141) Suslick, K. S.; Fang, M.; Hyeon, R.; Cichowlas, A. A. *Mater. Res. Soc. Symp. Proc.* **1994**, *351*, 443.
(142) Chow, G.-M.; Markowitz, M. A.; Singh, A. *JOM* **1993**, *5*, 62.
(143) Singh, A.; Markowitz, M. A.; Chow, G.-M. *Mater. Res. Soc. Symp. Proc* **1994**, *351*, 67.
(144) Singh, A.; Markowitz; M. A.; Chow, G. M. *Nanostruct. Mater.* **1995**, *5*, 141.
(145) Heuer, A.; Fink, D. J.; Laraia, V. J.; Arias, J. L.; Calvert, P. D.; Kendall, K.; Messing, G. L.; Blackwell, J.; Rieke, P. C.; Thompson, D. H.; Wheeler, A. P.; Veis, A.; Caplan, A. I. *Science* **1992**, *255*, 1098.
(146) Chen, J. P.; Lee, K. M.; Sorensen, C. M.; Klabunde, K. J. Hadjipanayis, G. C *J. Appl. Phys.* **1994**, *75*, 5876.
(147) Chen, J. P.; Sorensen, C. M.; Klabunde, K. J.; Hadjipanyis, G. C. *Phys. Rev. B* **1995**, *51*, 11527.
(148) Rivas, J.; López-Quintela, M. A.; López-Pérez, J. A.; Liz, L.; Duro, R. J. *IEEE Trans. Magn.* **1993**, *29*, 2655.
(149) Venturini, E. L.; Wilcoxon, J. P.; Newcomer, P. P. *Mater. Res. Soc. Symp. Proc.* **1994**, *351*, 322.
(150) Birringer, R.; Gleiter, H.; Klein, H.-P.; Marquardt, P. *Phys. Lett.* **1984**, *102A*, 365.
(151) Gleiter, H. *Deformation of Polycrystals: Mechanisms and Microstructures*; Hansen, N., et al., Eds.; Risø National Laboratory: Roskidle, 1981.
(152) Siegel, R. W.; Hahn, H. *Current Trends in the Physics of Materials*; Yussouff, M., Ed.; World Scientific: Singapore, 1987.
(153) Siegel, R. W.; Ramasamy, S.; Hahn, H.; Li, Z.; Lu, T.; Gronsky, R. *J. Mater. Res.* **1988**, *3*, 1367.
(154) Langvagen, S. Ye.; Lyubashevskiy, O. P.; Chizhov, P. Ye. *Phys. Met. Metall.* **1991**, *72*, 64.
(155) Falicov, L. M.; Pierce, D. T.; Bader, S. D.; Gronsky, R.; Hathaway, K. B.; Hopster, H. J.; Lambeth, D. N.; Parkin, S. S. P.; Prinz, G.; Salamon, M.; Schuller, I. K.; Victora, R. H. *J. Mater. Res.* **1990**, *5*, 1299.
(156) Childress, J. R.; Chien, C. L. *Appl. Phys. Lett.* **1990**, *56*, 95.
(157) Chien, C. L.; Liou, S. H.; Kofalt, D.; Yu, W.; Egami, T.; McGuire, T. R. *Phys. Rev. B* **1986**, *33*, 3247.
(158) Koch, C. C. *Annu. Rev. Mater. Sci.* **1989**, *19*, 121.
(159) Koch, C. C. *Nanophases and Nanocrystalline Structures*; Shull, R. D., Sanchez, J. M., Eds.; *TMS*, **1994**.
(160) Koch, C. C. *Nanostruct. Mater.* **1993**, *2*, 109.
(161) McHenry, M. E.; Majetich, S. A.; DeGraef, M.; Artman, J. O.; Staley, S. W. *Phys. Rev. B* **1994**, *49*, 11358.
(162) McHenry, M. E.; Nakamura, Y.; Kirkpatrick, S.; Johnson, F.; Majetich, S. A.; Brunsman, E. M. *Fullerenes: Physics, Chemistry, and New Directions VI*; Ruoff, R. S., Kadish, K. M., Eds.; The Electrochemical Society: Pennington, NJ, 1463, 1994.
(163) Majetich, S. A.; Artman, J. O.; McHenry, M. E. *Phys. Rev.* B **1993**, *48*, 16845.
(164) Lu, K.; Wang, J. T.; Wei, W. D. *J. Appl. Phys.* **1991**, *69*, 522.
(165) Herzer, G. *J. Magn. Magn. Mater.* **1992**, *112*, 258.
(166) Lu, K.; Wei, W. D.; Wang, J. T. *J. Appl. Phys.* **1991**, *69*, 7345.
(167) Yoshizawa, Y.; Oguma, S.; Yamauchi, K. J. *J. Appl. Phys* **1988**, *64*, 6044.
(168) Gibson, C. P.; Putzer, K. J. *Science* **1995**, *267*, 1338.
(169) Gangopadhyay, S.; Hadjipanayis, G. C.; Sorensen, C. M.; Klabunde, K. J. *IEEE Trans. Magn.* **1993**, *29*, 2602.
(170) Gangopadhyay, S.; Hadjipanayis, G. C.; Sorensen, C. M.; Klabunde, K. J. *IEEE Trans. Magn.* **1993**, *29*, 2619.
(171) Li, Y.; Gong, W.; Hadjipanyis, G. C.; Sorensen, C. M.; Klabunde, K. J.; Papaefthymiou, V.; Kostikas, A.; Simopoulos, A. *J. Magn. Magn. Mater.* **1994**, *130*, 261.
(172) Gong, W.; Li, H.; Zhao, Z.; Hadjipanayis, G. C.; Papaefthymiou, C. P.; Kostikas, A.; Simopouos, A. *J. Appl. Phys.* **1991**, *70*, 5900.
(173) Pankhurst, Q. A.; Pollard, R. J. *J. Phys.: Condens. Matter* **1993**, *5*, 8487.
(174) Jones, H. E.; Bissell, P. R.; Chantrell, R. W. *J. Magn. Magn. Mater.* **1990**, *83*, 445.
(175) Kaczmarek, W. A.; Calka, A.; Ninjam, B. W. *IEEE Trans. Magn.* **1993**, *29*, 2649.
(176) Davies, K. J.; Wells, S.; Upadhyay, R. V.; Charles, S. W.; O'Grady, K.; El-Hilo, M.; Meaz, T.; Mørup, S. *J. Magn. Magn. Mater.* **1995**, *149*, 14.
(177) Luo, H. L.; Wang, G. H. *J. Magn. Magn. Mater.* **1994**, *129*, 389.
(178) Pfeiffer, H.; Schüppel, W. *J. Magn. Magn. Mater.* **1994**, *130*, 92.
(179) Bottoni, G. *IEEE Trans. Magn.* **1993**, *29*, 2661.
(180) Tang, Z. X.; Sorensen, C. M.; Klabunde, K. J.; Hadjipanayis, G. C. *J. Appl. Phys.* **1991**, *69*, 5279.
(181) Tang, Z. X.; Sorensen, C. M.; Klabunde, K. J.; Hadjipanayis, G. C. *Phys. Rev. Lett.* **1991**, *67*, 3602.
(182) Nishio, H.; Taguchi, H.; Hirata, F.; Takeishi, T. *IEEE Trans. Magn.* **1993**, *29*, 2637.
(183) Ram, S.; Joubert, J. C. *Phys. Rev. B* **1991**, *44*, 6825.
(184) El-Hilo, M.; Pfeiffer, H.; O'Grady, K.; Schüppel, W.; Sinn, E.; Görnert, P.; Rösler, M.; Dickson, D. P. E.; Chantrell, R. W. *J. Magn. Magn. Mater.* **1994**, *129*, 339.
(185) Ho, J. C.; Hamdeh, H. H.; Chen, Y. Y.; Lin, S. H.; Yao, Y. D.; Willey, R. J.; Oliver, S. A. *Phys. Rev. B* **1995**, *52*, 10122.
(186) Zahn, S. A.; Shenton, K. E. *IEEE Trans. Magn.* **1980**, *16*, 387.
(187) Söffge, F.; Schmidbauer, E. *J. Magn. Magn. Mater.* **1981**, *24*, 54.
(188) Mørup, S. *Europhys. Lett.* **1994**, *28*, 671.
(189) Linderoth, S.; Hendriksen, P. V.; Bødker, F.; Wells, S.; Davies, K.; Charles, S. W. Mørup, S. *J. Appl. Phys.* **1994**, *75*, 6583.
(190) Mørup, S.; Bødker, F.; Hendriksen, P. V.; Linderoth, S. *Phys. Rev. B* **1995**, *52*, 287.
(191) Zaleska-Kotur, M. A.; Cieplak, M. *Europhys. Lett.* **1993**, *23*, 85.
(192) Jen, S. U.; Lee, C. Y.; Yao, Y. D.; Lee, K. C. *J. Magn. Magn. Mater.* **1991**, *96*, 82.
(193) Dimitrov, D. A.; Wysin, G. M. *Phys. Rev. B* **1994**, *50*, 3077.
(194) Meriloski, J.; Timonen, J.; Manninen, M.; Jena, P. *Phys. Rev. Lett.* **1991**, *66*, 938.
(195) Kanna, S. N.; Linderoth, S. *Phys. Rev. Lett.* **1991**, *67*, 742.
(196) Linderoth, S.; Khanna, S. N. *J. Magn. Magn. Mater.* **1992**, *104−107*, 1574.
(197) Gangopadhyay, S.; Hadjipanayis, G. C.; Shah, S. I.; Sorensen, C. M.; Klabunde, K. J.; Papaefthymiou, V.; Kostikas, A. *J. Appl. Phys.* **1991**, *70*, 5888.
(198) Gangopadhyay, S.; Hadjipanayis, G. C.; Dale, B. D.; Sorensen, C. M.; Klabunde, K. J.; Papaefthymiou, V.; Kostikas, A. *Phys. Rev. B* **1992**, *45*, 9778.
(199) Gangopadhyay, S.; Hadjipanayis, G. C.; Sorensen, C. M.; Klabunde, K. J. *J. Appl. Phys.* **1993**, *73*, 6964.
(200) Arrott, A. S.; Templeton, T. L.; Yoshida, Y. *IEEE Trans. Magn.* **1993**, *29*, 2622.
(201) Darnell, F. J. *J. Appl. Phys.* **1961**, *32*, 186S.
(202) Falk, R. B.; Hooper, G. D. *J. Appl. Phys.* **1961**, *32*, 190S.
(203) Kishimoto, M.; Nakazumi, T.; Otani, N.; Sueyoshi, T. *IEEE Trans. Magn.* **1991**, *27*, 4645.
(204) Uchikoshi, T.; Sakka, Y.; Yoshitake, M.; Yoshihara, K. *Nanostruct. Mater.* **1994**, *4*, 199.
(205) Yao, Y. D.; Chen, Y. Y.; Hsu, C. M.; Lin, H. M.; Tung, C. Y.; Tai, M. F.; Wang, D. H.; Wu, K. T.; Suo, C. T. *Nanostruct. Mater.* **1995**, *6*, 933.
(206) Yiping, L.; Hadjipanyayis, G. C.; Sorensen, C. M.; Klabunde, K. J. *J. Appl. Phys.* **1994**, *75*, 5885.
(207) Otani, Y.; Miyajima, H.; Yamaguchi, M.; Nozaki, Y.; Fagan, A.J.; Coey, J. M. D. *J. Magn. Magn. Mater.* **1994**, *135*, 293.
(208) Lin, H.-M.; Hsu, C. M.; Yao, Y. D.; Chen, Y. Y.; Kuan, T. T.; Yang, F. A.; Tung, C. Y. *Nanostruct. Mater.* **1995**, *6*, 977.
(209) Templeton, T. L.; Yoshida, Y.; Li, X.-Z.; Arrott, A. S.; Curzon, A. E.; Hamed, F.; Gee, M. A.; Schurer, P. J.; LaCombe, J. L. *IEEE Trans. Magn.* **1993**, *29*, 2625.
(210) Nicklasson, G. A.; Granquist, C. G. *J. Appl. Phys.* **1984**, *55*, 3382.
(211) Schlesinger, T. E.; Cammarata, R. C.; Gavrin, A.; Chien, C. L.; Ferber, M. F.; Hayzelden, C. *J. Appl. Phys.* **1991**, *70*, 3275.
(212) Gavrin, A.; Chien, C. L. *J. Appl. Phys.* **1990**, *67*, 938.
(213) Paparazzo, E.; Dormann, J. L.; Fiorani, D. *Phys. Rev. B* **1983**, *28*, 1154.
(214) Dormann, J. L.; Djega-Mariadassou, C.; Jove, J. *J. Magn. Magn. Mater.* **1992**, *104−107*, 1567.
(215) Djega-Mariadassou, C.; Dormann, J. L.; Noguès, M.; Villers, G.; Sayouri, S. *IEEE Trans. Magn.* **1990**, *26*, 1819.
(216) Gittleman, J. L.; Goldstein, Y.; Bozowski, S. *Phys. Rev. B* **1972**, *5*, 3609.
(217) Gittleman, J. I.; Abeles, B.; Bozowski, S. *Phys. Rev. B* **1974**, *9*, 3891.
(218) Childress, J. R.; Chien, C. L. *Appl. Phys. Lett.* **1990**, *56*, 95.
(219) Chien, C. L.; Liou, S. H.; Kofalt, D.; Yu, Wu; Egami, T.; McGuire, T. R. *Phys. Rev. B* **1986**, *33*, 3247.
(220) Shull, R. D.; Ritter, J. J.; Shapiro, A. J.; Swartzendruber, L. J.; Bennett, L. H. *Mater. Res. Soc. Symp. Proc.* **1989**, *132*, 179.
(221) Wang, J.-P.; Han, D.-H.; Luo, H.-L.; Gao, N.-F.; Liu, Y.-Y. *J. Magn. Magn. Mater.* **1994**, *135*, L251.
(222) Ambrose, T.; Gavrin, A.; Chien, C.-L. *J. Magn. Magn. Mater.* **1992**, *116*, L311.
(223) Pardavi-Horvath, M.; Takacs, L.; Cser, F. *IEEE Trans. Magn.* **1995**, *31*, 3775.
(224) Takacs, L.; Pardavi-Horvath, M. *J. Appl. Phys.* **1994**, *75*, 5864.
(225) Liu, Y.; Dallimore, M. P.; McCormick, P. G.; Alonso, T *J. Magn. Magn. Mater.* **1992**, *116*, L320.
(226) Pardavi-Horvath, M.; Takacs, L. *J. Appl. Phys.* **1993**, *73*, 6958.
(227) Zeltser, A. M.; Soffa, W. A. *J. Appl. Phys.* **1990**, *67*, 6958.
(228) Shpeizer, B.; Poojary, D. M.; Ahn, Kyungsoo; Runyan, Jr., C., E.; Clearfield, A. *Science* **1994**, *266*, 1357.
(229) Pinheiro, M.; Rosenberg, H. M. *J. Polym. Sci., Polym. Phys. Ed.* **1980**, *18*, 217.
(230) Hudak, O. *Czech. J. Phys.* **1986**, *B35*, 1303.
(231) Hyeon, T.; Suslick, K. S. Presentation COLL 069, 210th American Chemical Society Meeting, Chicago, August, 1995.
(232) Nikles, D. E.; Cain, Jason L.; Chacko, Ap. P.; Webb, R. I. *IEEE Trans. Magn.* **1995**, *30*, 4068.

(233) Laurent, C.; Mauri, D.; Kay, E.; Parkin, S. S. P. *J. Appl. Phys.* **1989**, *65*, 2017.
(234) Leslie-Pelecky, Diandra, L.; Zhang, X. Q.; Rieke, R. D. *J. Appl. Phys.* **1996**, *79*, 5312.
(235) Ziolo, R. F.; Giannelis, E. P.; Shull, R. D. *NanoStruct. Mater.* **1993**, *3*, 85.
(236) Vassiliou, J. K.; Mehrotra, V.; Russell, M. W.; Giannelis, E. P. *Mater. Res. Soc. Symp. Proc.* **1991**, *206*, 561.
(237) Marchessault, R. H.; Ricard, S.; Rioux, P. *Carbohyr. Res.* **1992**, *224*, 133.
(238) El-Awansi, A.; Kinawy, N.; Emitwally, M. *J. Mat. Sci.* **1989**, *24*, 2497.
(239) Göktürk, Halit, S.; Fiske, Thomas, J.; Kalyon, Dilhan, M. *J. Appl. Poly. Sci.***1993**, *50*, 1891.
(240) Yacubowicz, J.; Narkis, M. *Poly. Eng., & Sci.* **1990**, *30*, 469.
(241) O'Brian, Richard; Rieke, Reuben, D. *J. Org. Chem*, **1990**, *55*, 755.
(242) O'Brian, Richard; Rieke, Reuben, D. *J. Org. Chem*. **1992**, *57*, 2667.
(243) Bean, C. P.; Livingston, J. D. Rodbell, D. S. *J. Phys. Rad*. **1956**, *20*, 298.
(244) Illenberger, A.; Numez, L. J. *Z. Phys. Chem*. **1960**, *23*, 145.
(245) Lázaro, F. J.; García, J. L.; Schünemann, V.; Trautwein, A. X. *IEEE Trans. Magn.* **1993**, *29*, 2652.
(246) Diandra, L. Leslie-Pelecky, X. Q. Zhang, G. L. Krichau, B. W. Robertson and Reuben D. Rieke, *Proceedings of the American Chemical Society Division of Polymeric Materials: Science and Engineering*, **1995**, *73*, 66.
(247) Hooker, P.; Tan, B. J.; Klabunde, K. J.; Suib, S. *Chem. Mater.* **1991**, *3*, 947.
(248) Pauthenet, R. *J. Appl. Phys.* **1982**, *53*, 2031.
(249) Kisker, H.; Gessmann, T.; Würschum, R.; Kronmüller, H.; Schaefer, H.-E. *Nanostruct. Mater.* **1995**, *6*, 925.
(250) Birringer, R.; Herr, U.; Gleiter, H. *Suppl. Trans. Jpn. Inst. Met.* **1986**, *27*, 43.
(251) Daróczi, L.; Beke, D. L.; Posgay, G.; Zhou, G. F.; Bakker, H. *Nanostruct. Mater.* **1993**, *2*, 515.
(252) Daróczi, L.; Beke, D. L.; Posgay, G.; Kis-Varga, M. *Nanostruct. Mater.* **1995**, *6*, 981.
(253) Hirscher, M.; Reisser, R.; Würschum, R.; Schaefer, H.-E.; Kronmüller, H. *J. Magn. Magn. Mater.* **1995**, *146*, 117.
(254) Kronmüller, H.; Schrefl, T. *J. Magn. Magn. Mater.* **1994**, *129*, 66.
(255) Herzer, G.; Warlimont, H. *Nanostruct. Mater.* **1992**, *1*, 263.
(256) Reininger, T.; Hofmann, B.; Krönmuller, H. *J. Magn. Magn. Mater.* **1992**, *111*, L220.
(257) Coehoorn, R.; DeMooij, D. B.; DeWaard, C. *J. Magn. Magn. Mater.* **1989**, *81*, 109.
(258) Coehoorn, R.; DeMooij, D. B.; Duchateau, J. P. W. B.; Buschow, K. H. J. *J. Phys. (Paris)* **1988**, *C8*, 669.
(259) Manaf, A.; Buckley, R. A.; Davies, H. A. *J. Magn. Magn. Mater.* **1993**, *128*, 302.
(260) Schultz, L.; Schnitzke, K.; Wecker, J.; Katter, M.; Kuhrt, C. *J. Appl. Phys.* **1991**, *70*, 6339.
(261) Schultz, L.; Wecker, J.; Hellstern, E. *J. Appl. Phys.* **1987**, *61*, 3585.
(262) Koestler, C.; Ramesh, R.; Echner, C. J.; Thomas, G.; Wecker, J. *Acta Metall.* **1989**, *37*, 1945.
(263) Davies, H. A.; Manaf, A.; Leonowicz, M.; Zhang, P. Z.; Dobson, S. J.; Buckley, R. A. *Nanostruct. Mater.* **1993**, *2*, 197.
(264) den Broeder, F. J. A.; Buschow, K. H. J. *J. Less-Common Met.* **1972**, *29*, 67.
(265) Wecker, J.; Katter, M.; Schultz, L. *J. Appl. Phys.* **1991**, *69*, 6058.
(266) Niessen, A. K.; de Broer, F. R.; Boom, R.; de Chatel, P. F.; Mattens, C. W. M.; Miedema, R. A. *Calphad* **1986**, *7*, 51.
(267) Ding, J.; McCormick, P. G.; Street, R. *J. Magn. Magn. Mater.* **1995**, *135*, 200.
(268) Katter, M.; Wecker, J.; Schultz, L. *J. Appl. Phys.* **1991**, *70*, 3188.
(269) Furrer, P.; Warlimont, H. *Mater. Sci. Eng.* **1977**, *28*, 12.
(270) O'Handley, R. C.; Megusar, J.; Sun, S. W.; Hara, Y.; Grant, N. J. *J. Appl. Phys.* **1986**, *57*, 3563.
(271) Liu, Y.; Dallimore, P.; McCormick, P. G. *Appl. Phys. Lett.* **1992**, *60*, 3136.
(272) Ding, J.; Liu, Y.; McCormick, P. G.; Street, R. *J. Magn. Magn. Mater.* **1993**, *123*, L239.
(273) Schalek, R. L.; Leslie-Pelecky, D. L.; Knight, J.; Sellmyer, D. J.; Axtell, S. C. *IEEE Trans. Magn.* **1995**, *31*, 3772.
(274) Al-Omari, I. A.; Sellmyer, D. J. *Phys. Rev. B* **1995**, *52*, 3441.
(275) Kneller, E.; Hawig, R. *IEEE Trans. Magn.* **1991**, *27*, 3588.
(276) Skomski, R.; Coey, J. M. D. *Phys. Rev. B* **1993**, *48*, 15812.
(277) Schrefl, T.; Kronmuller, H.; Fidler, J. *J. Magn. Magn. Mater.* **1993**, *127*, L271.
(278) Schrefl, T.; Fischer, R.; Fidler, J.; Kronmuller, H. *J. Appl. Phys.* **1994**, *76*, 7053.
(279) Fukunaga, H.; Inoue, H.; *Jpn. J. Appl. Phys.* **1992**, *31*, 1347.
(280) Clemente, G. B.; Keen, J. E.; Bradley, J. P. *J. Appl. Phys.* **1988**, *64*, 5299.
(281) Fitzsimmons, M. R.; Röll, A.; Burkel, E.; Sikafus, K. E.; Nastasi, M. A.; Smith, G. S.; Pynn, R. *J. Appl. Phys.* **1994**, *76*, 6295.
(282) Martin, C. R. *Science* **1994**, *266*, 1961.
(283) Chlebny, I.; Doudin, B.; Ansermet, J. Ph. *Nanostruct. Mater.* **1993**, *2*, 637.
(284) Cai, Z.; Martin, C. R. *J. Am. Chem. Soc.* **1989**, *111*, 4138.
(285) Piraux, L.; George, J. M.; Despres, J. F.; Leroy, C.; Ferain, E.; Legras, R.; Ounadjela, L.; Fert, A. *Appl. Phys. Lett.* **1994**, *65*, 2483.

CM960077F